NATIONAL AERONAUTICS AND SPACE ADMINISTRATION

Technical Report 32-1268

An Evaluation of Photovoltaic Devices for Future Spacecraft Power Demands

D. W. Ritchie
J. D. Sandstrom

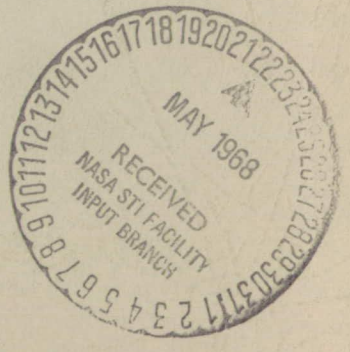

JET PROPULSION LABORATORY
CALIFORNIA INSTITUTE OF TECHNOLOGY
PASADENA, CALIFORNIA

May 1, 1968

NATIONAL AERONAUTICS AND SPACE ADMINISTRATION

Technical Report 32-1268

An Evaluation of Photovoltaic Devices for Future Spacecraft Power Demands

D. W. Ritchie
J. D. Sandstrom

Approved by:

L. D. Runkle, *Assistant Manager*
Spacecraft Power Section

JET PROPULSION LABORATORY
CALIFORNIA INSTITUTE OF TECHNOLOGY
PASADENA, CALIFORNIA

May 1, 1968

Contents

Tables

Figures

Contents (contd)

Figures (contd)

Abstract

The present trend of photovoltaic power systems is toward power levels in excess of 1 kW and specific power levels of 50 lb/kW, or less. The workhorse of the photovoltaic systems, to date, has been the silicon solar cell; the largest, to date, in a spacecraft power system has been 4 cm^2. Future systems using photovoltaics may find it advantageous to use devices with greater active area and lighter weight; however, the conventional size cell (2- × 2-cm) will probably be the only ones available for the next several years. There are two photovoltaic devices under development that will satisfy larger active area requirements—the cadmium sulphide cell and the dendritic-type silicon cell. Each of these cell developments is approaching a technology level that is nearly competitive with conventional silicon cell capabilities. This paper compares the various cell types and presents discussion as to the potential advantages or disadvantages of each for system usage.

An Evaluation of Photovoltaic Devices for Future Spacecraft Power Demands

I. Introduction

The increased interest in photovoltaics for spacecraft power systems is due to the potential of solar cells for satisfying spacecraft power demands to multikilowatt levels. Photovoltaic development activities today are centered around the more promising devices, such as the thin silicon single-crystal solar cell, the webbed dendritic polycrystalline solar cell, and the flexible-film cadmium sulphide (CdS) cell. The potential offered by these various photovoltaic devices and the generally favorable results of advanced studies utilizing photovoltaics in high-power systems has led to some optimism concerning their applications.

To more fully evaluate the potential of these various devices, data are presented on the electrical characteristics of the three cell types listed above. Also, consideration is given to applying the various cells to solar array systems. This paper reports work performed at the Jet Propulsion Laboratory to evaluate the potentials of photovoltaic devices under development by the NASA and the USAF. The data include electrical evaluation of cell parameters in the intensity and temperature environments between 0.7 and 5.0 astronomical units (AU).

II. Present Technology

A. Single-Crystal Silicon Solar Cells

The single-crystal silicon solar cell has been the prime photovoltaic device used in spacecraft power systems for the past 10 yr. This solar-energy converter has demonstrated its capabilities in space environments between 0.7 and 1.6 AU. The present single-crystal solar cell used in spacecraft design is the *n-p* type silicon cell. This cell polarity has produced a more radiation-resistant output characteristic than the *p-n* silicon cell used in many of the earlier power conversion flight programs. It should be noted however, that an *a priori* selection of *n-p* over *p-n* type cell, because of its increased radiation resistance, may prove fallacious for *all* types of deep space missions, particularly those involving elevated array temperature.

The silicon cell presently used in spacecraft designs has a nominal thickness of 0.012 in. and is constructed with evaporated silver-titanium solder-coated contacts. The power capability of this cell in a sun oriented solar array at 1 AU is about 10 W/ft^2 and 10 W/lb. The weight breakdown of the array system is 50% for cells, wiring, filtering (0.006 in.), and adhesive; the remaining 50% is support structure, deployment mechanisms, and thermal coating. The individual unassembled solar cell efficiency at air mass zero (AM0) is 11% at a cell temperature of 28°C.

The most widely used method to produce silicon solar cells is from grown cylindrical single-crystals of silicon, which are cut to rectangular blocks, sliced, lapped, and then gas-diffused to form solar cells.

B. Webbed Dendritic Polycrystalline Silicon Solar Cells

By the process of webbed dendritic growth, long, thin, polycrystalline strips of silicon can be grown. Presently, the webbed dendritic solar cell is in the pilot production stage. These cells are nominally 0.012 in. thick and can be procured in lengths up to 30×1 cm. The electrical contact to the cell is solderless silver-titanium. The electrical efficiency of the cell, as quoted by the manufacturer, is about 10% at AM0, at a cell temperature of 28°C. The development of the dendritic-type cell has been sponsored by the Air Force Aero Propulsion Laboratory, WPAFB. The webbed dendritic solar cell has only been used in experimental capacities to date.

C. Cadmium Sulphide Solar Cell

The cadmium sulphide solar cell has been under development since 1960–61. These development efforts have been sponsored by both the USAF and the NASA. The development of the CdS has led to a flexible-film type cell which can be produced in pilot line production with efficiencies of about 3.1% at AM0, 28°C. Problems of the CdS cell to date are related to stability and film material encapsulation. Presently, two films are used for cell encapsulation—Mylar and Kapton. Of these, the Kapton film currently produces the more stable type cell, with efficiencies slightly less than the Mylar system.

III. Cell Test System

To perform temperature-intensity parametric studies on solar cells, a thermal–vacuum solar simulator test facility was installed in the JPL photovoltaic developmental laboratory. The thermal–vacuum portion of the facility had been used previously in cell evaluation programs and has been modified appropriately to allow the testing of the various photovoltaic devices in use today. The solar simulator[1] was recently purchased specifically for cell investigations. The system is illustrated diagrammatically in Fig. 1.

The primary function of the vacuum chamber is to eliminate water condensation on the surface of cells when testing below 0°C. The vacuum chamber[2] uses a bell jar that is 23 in. long and 18 in. in diameter. A protruded portion of the bell jar is terminated in an 8-in.-diam quartz window, which faces the source. A vacuum of 5 μm is maintained by a Kinney roughing pump. A cold trap has been installed in the roughing line to minimize back-streaming from the pump.

A vertical test fixture is mounted within the bell jar on a lab jack, which is adjustable. The test fixture is constructed from channeled copper for the passage of liquid nitrogen, and a 350 W nichrome heating pad is sandwiched between the channeled fixture and a ⅛-in. copper plate, upon which test specimens are mounted. A West saturable core reactor, digital set-point temperature controller modulates the input power to the heating pad according to the demand, supplying more or less power to the load. When control temperature is reached, the heating pad receives only enough power to take care of temperature losses. The instrument is capable of controlling through the ranges of −100 to 200°C. The control point is set by turning a three-digit, 1,000-part dial. A continuous cold-junction compensation is provided electrically.

In this investigation, a copper constantan feed-through with 18 thermocouples was used to sense temperatures; six of the thermocouple junctions were mounted to different locations on the test fixture. These thermocouples were used primarily to monitor temperature gradients across the test fixture. Temperature was monitored continuously by an automatic 16-channel temperature recorder[3] in the range from −100 to 150°C.

The system includes an intensity reference cell that has been calibrated against JPL balloon standards. The intensity reference cell is mounted on a thermal-electric module (TE) which, in turn, is mounted to a water-cooled test fixture. This test fixture is isolated, thermally and electrically, from the main test fixture. Two copper

[1]Spectrolab X-25L.
[2]Manufactured by Consolidated Electrodynamics.
[3]Leeds and Northrup Speedomax, Type G.

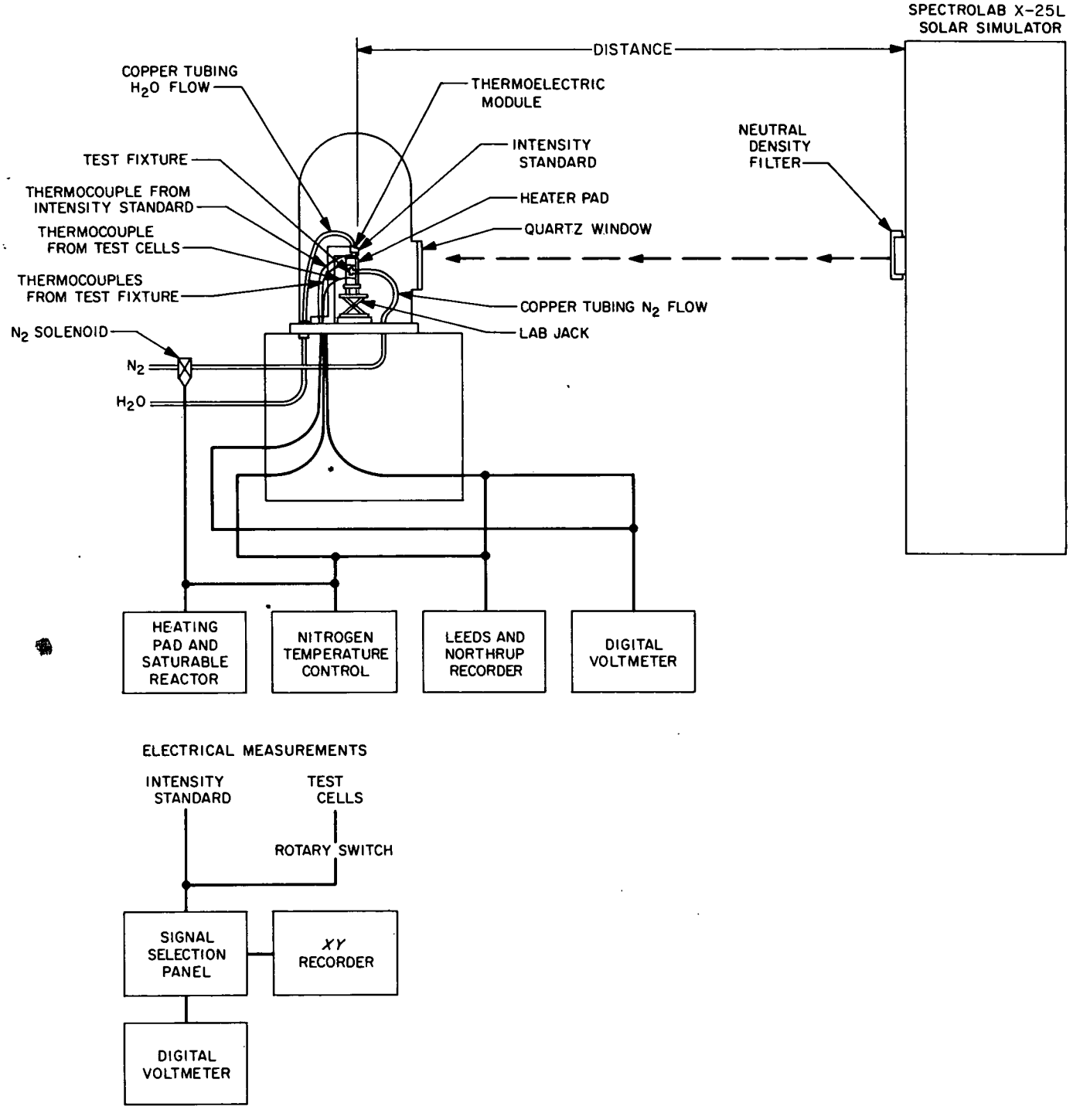

Fig. 1. Test system diagram

constantan thermocouples are imbedded in the mounting plate near the cell and are monitored with a digital-voltmeter to ensure that the intensity standard is maintained at a constant temperature of 28°C. This is accomplished by passing a quantity of direct current through the TE module from a regulated power supply; the amount required depends on the industrial water temperature and the amount of light energy incident upon the surface of the reference cell. The short-circuit current output from the intensity reference cell is established, at any given temperature, before and after electrical measurements are taken on the test specimens. Prior to the initiation of testing, this cell was carefully calibrated to serve as an intensity standard from 250 mW/cm^2 to 5 mW/cm^2 equivalent space sunlight intensity.

The light source used in these investigations is a solar simulator that utilizes a 19-lens lenticular system to filter a 2.5 kW xenon source such that the resultant spectral distribution approaches that of space sunlight. The light source is calibrated using various solar cells that JPL has flown (during the past 6 yr) on high-altitude balloons, in conjunction with the solar cell standardization program. These calibrated cells fit into several categories: those that were unfiltered, those filtered with a 0.41 μm cutoff interference filter, those with bandpass filters (approximately 0.1 μm transmission), and those that were filtered to pass energy in the infrared or ultraviolet portions of the solar spectrum. Table 1 presents a listing of the cells that were used to calibrate the source, showing the deviation from the cells AM0 output (short-circuit current) and it's output under one sun illumination from the solar simulator. The solar simulator appears to be approximately 4% rich in the ultraviolet portion and 5% poor in the infrared portion of the spectrum, in the regions of silicon solar cell response. However, the unfiltered balloon standard cells and those that were filtered with a standard 410Å cutoff interference filter showed a short-circuit current correlation to within 1.5%.

Table 1. Simulator calibration

Number of cells tested	Filter wavelength, μm	Average deviation from flown reading, %
2	Red	— 4.66
2	Blue	+ 3.55
9	None	± 0.58
1	0.4 - 0.5	+11.49
1	0.5 - 0.6	+ 0.68
1	0.6 - 0.7	+ 1.51
1	0.7 - 0.8	— 7.09
1	0.8 - 0.9	—18.93
1	0.9 - 1.1	+ 2.92
10	0.410 cutoff	— 1.45
2	0.410 cutoff (radiated)	— 4.93

The complete system used to illuminate and measure the various cell types investigated in this study is shown in Fig. 2. Presented in Fig. 3 are typical solar cell test plates that mount on the vertical test fixture in the thermal–vacuum chamber. All of the cells employed during this test program were mounted, using a four-point electric circuit, and are bonded to the copper plates with RTV 40 silicone adhesive.

The test procedure for each type cell included illumination at space equivalent flux levels of 250, 200, 140, 100, 50, 25, 15, and 5 mW/cm^2. The cell temperature was varied from 60 to −40°C in 20° increments at each intensity level. In addition, some cell types were evaluated at temperatures to 100°C and as low as −140°C at several intensities. Tabulated in Table 2 are the cell types, number of cells, and ranges of intensity and temperature investigated for each cell type.

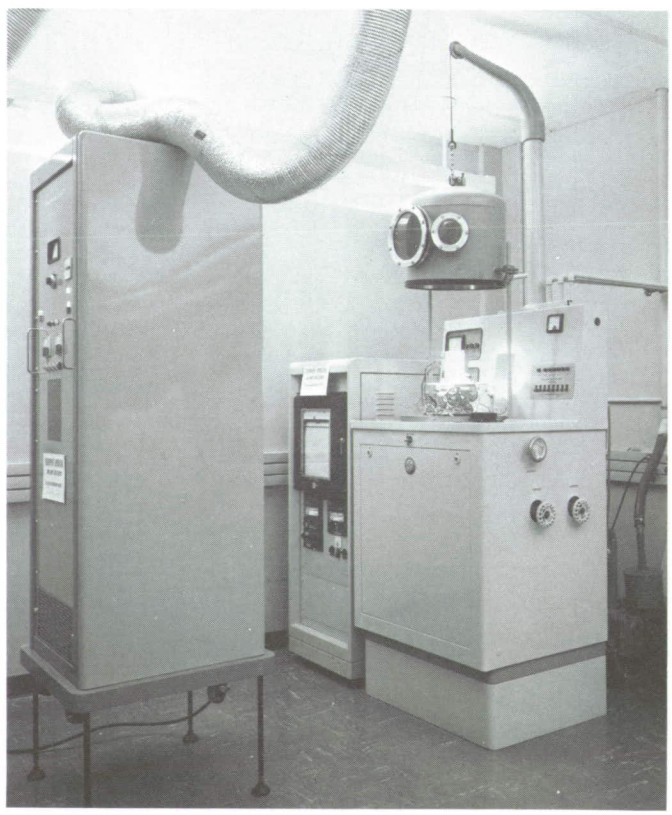

Fig. 2. Thermal-vacuum test facility

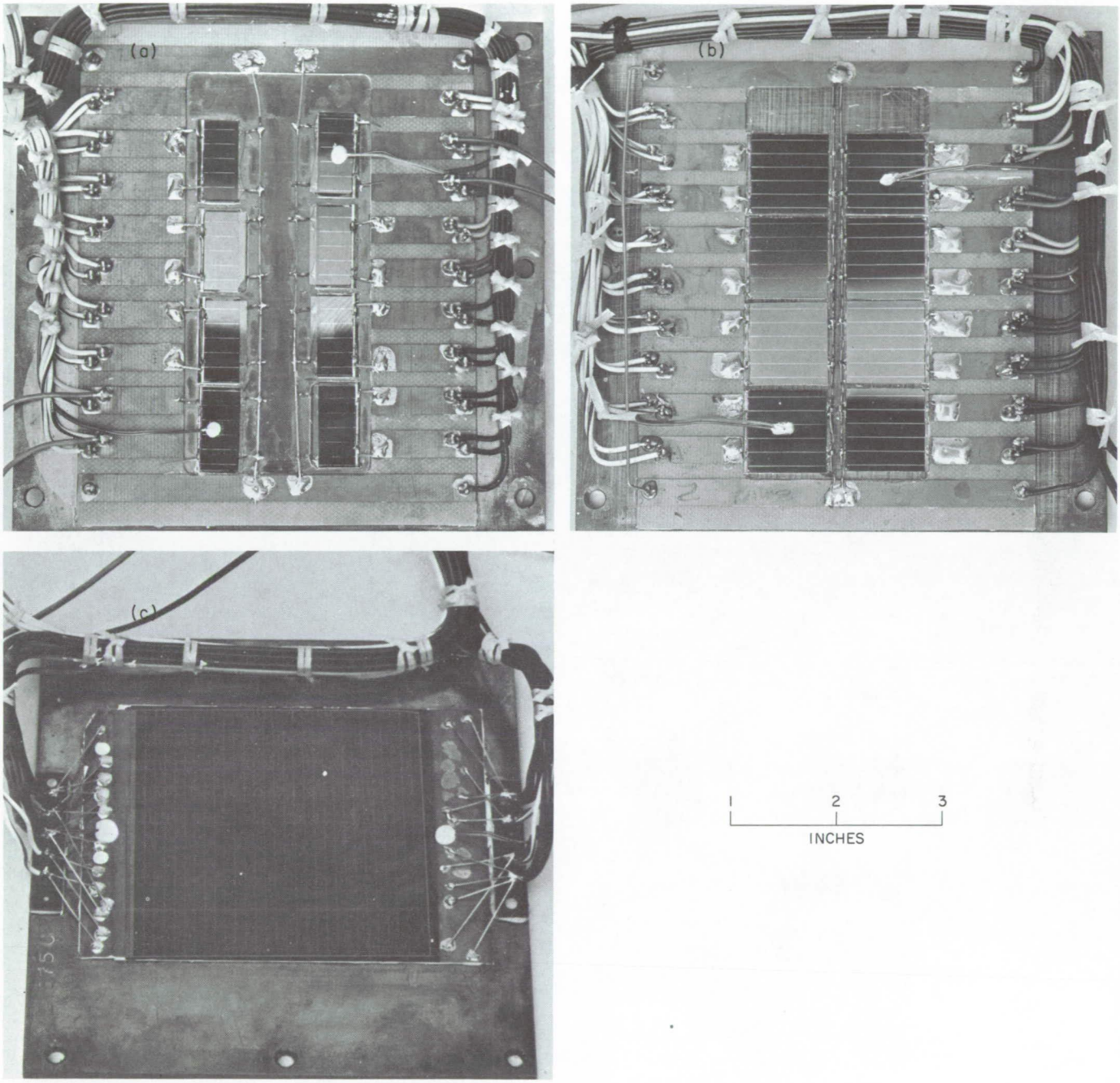

Fig. 3. Three cell types tested

Table 2. Description of cells and experiment

Cell type	Nominal base resistivity, Ω-cm	Thickness, in.	Number of cells tested	Intensity, mW/cm²	Temperature range, °C
n-p silicon 2 x 2 cm	2	0.008	12	250	−40 to 100
				140	−40 to 100
				100	−40 to 60
				50	−40 to 60
				25	−40 to 60
				5	−80 to 60
n-p silicon 2 x 2 cm	2	0.018	12	250	−40 to 100
				140	−40 to 100
				100	−40 to 60
				69	−40 to 60
				25	−100 to 60
				5	−40 to 60
n-p dendritic 1 x 2 cm	2	0.012	6	250	−40 to 60
				140	−40 to 60
				25	−40 to 60
Thin-film CdS 3 x 3 in.		0.005	3	250	20 to 60
				140	−40 to 60
				25	−40 to 60

IV. Experimental Results

The mean cell parameters (short-circuit current, open-circuit voltage, maximum cell power and cell efficiency) of all the various cell types are presented in Figs. 4 through 21 as a function of solar intensity and cell temperature.

The short-circuit currents (I_{sc}) as a function of cell temperature for the 8- and 18-mil single-crystal silicon, dendritic silicon, and CdS solar cells are shown in Figs. 4, 8, 12, and 16, respectively. The short-circuit current increases linearly with temperature above 0°C for the

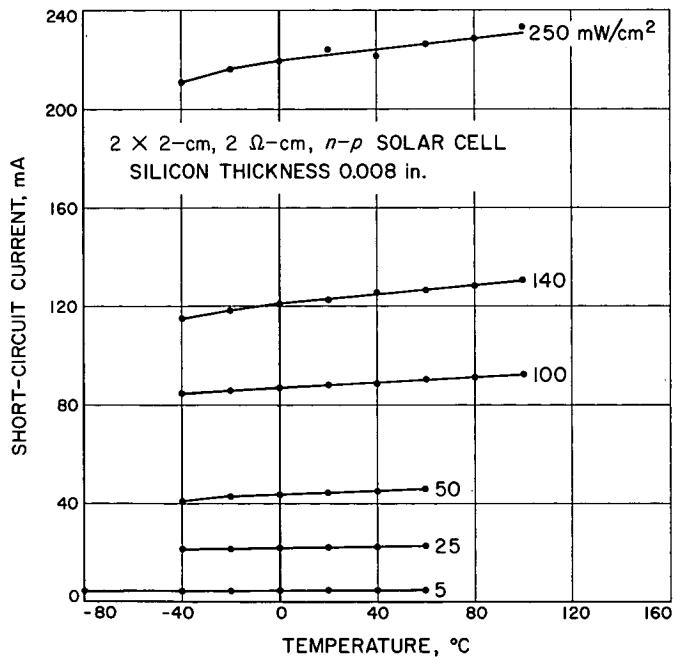

Fig. 4. Short-circuit current as a function of temperature for 8-mil single-crystal solar cell

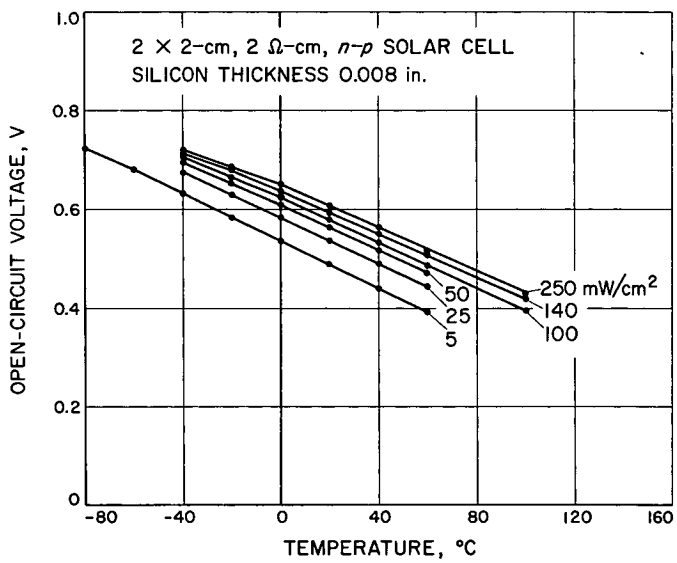

Fig. 5. Open-circuit voltage as a function of temperature for 8-mil single-crystal solar cell

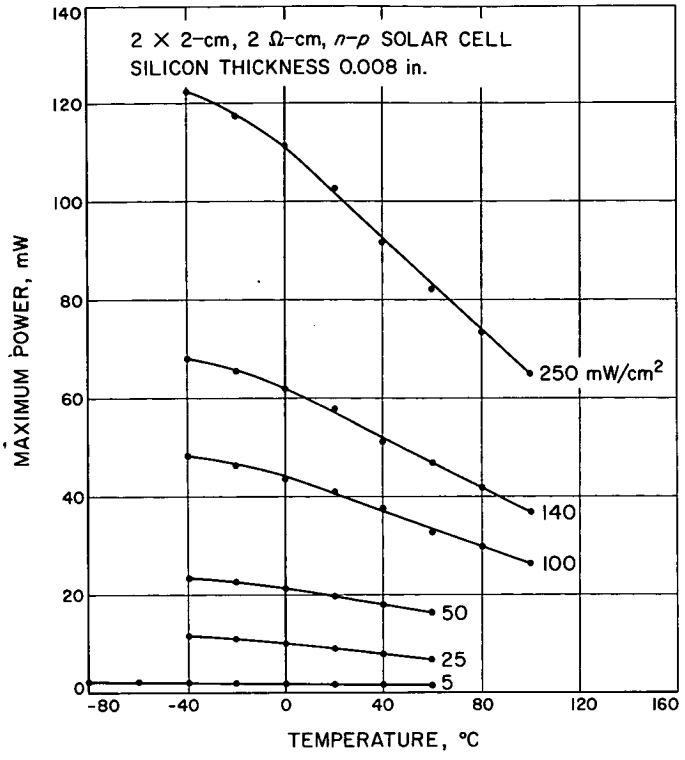

Fig. 6. Maximum power as a function of temperature for 8-mil single-crystal solar cell

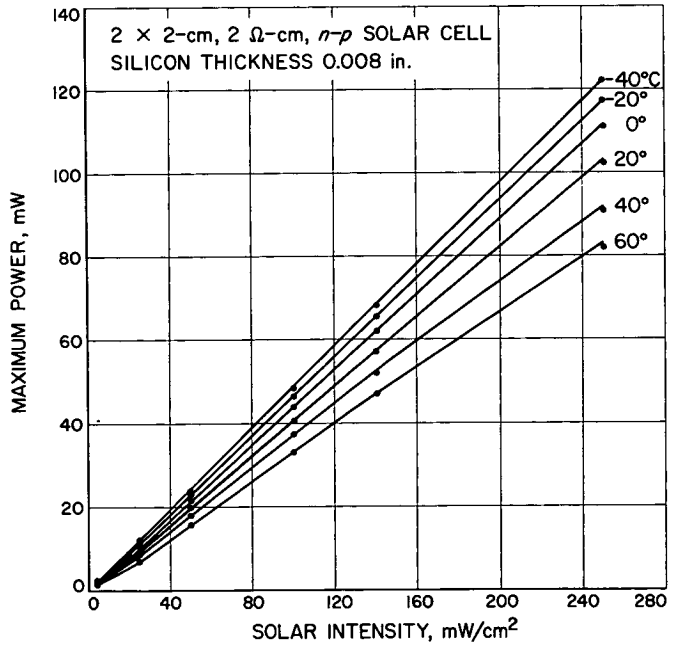

Fig. 7. Maximum power as a function of solar intensity for 8-mil single-crystal solar cell

silicon-type solar cells, but is essentially constant with temperature for the CdS type cell to 40°C. Above this temperature, the CdS current starts to decrease. This effect has not been observed in silicon solar cells for temperatures up to 120°C; however, the I_{sc} shows some non-linearity below 0°C. The short-circuit current as a function of the solar flux level, for any given temperature, increases linearly with solar intensity.

The open-circuit voltage (V_{oc}) as a function of cell temperature for the 8- and 18-mil single-crystal silicon, dendritic silicon, and CdS solar cells are shown in Figs. 5, 9, 13, and 17, respectively. The decreases in V_{oc} with increasing cell temperature is approximately linear above 0°C for every type cell investigated in this study. It was observed, however, that the open-circuit voltage does not increase linearly with temperature below 0°C. This open-circuit voltage nonlinearity is especially pronounced at 250 mW/cm² for the dendritic silicon type solar cells. The open-circuit voltage temperature coefficient at AM0 for the silicon (n-p) type solar cell is nominally 2.2 mV/°C and 1.3 mV/°C for the CdS solar cell.

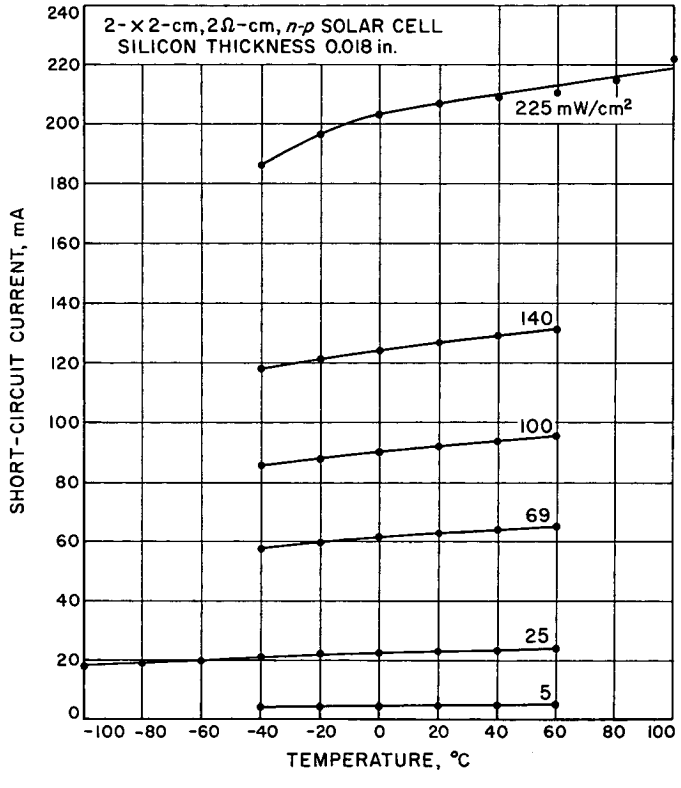

Fig. 8. Short-circuit current as a function of temperature for 18-mil single-crystal solar cell

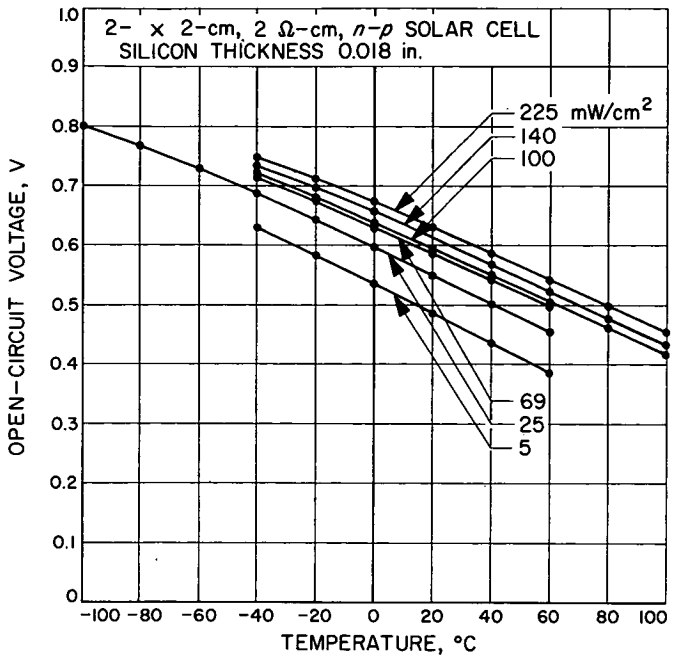

Fig. 9. Open-circuit voltage as a function of temperature for 18-mil single-crystal solar cell

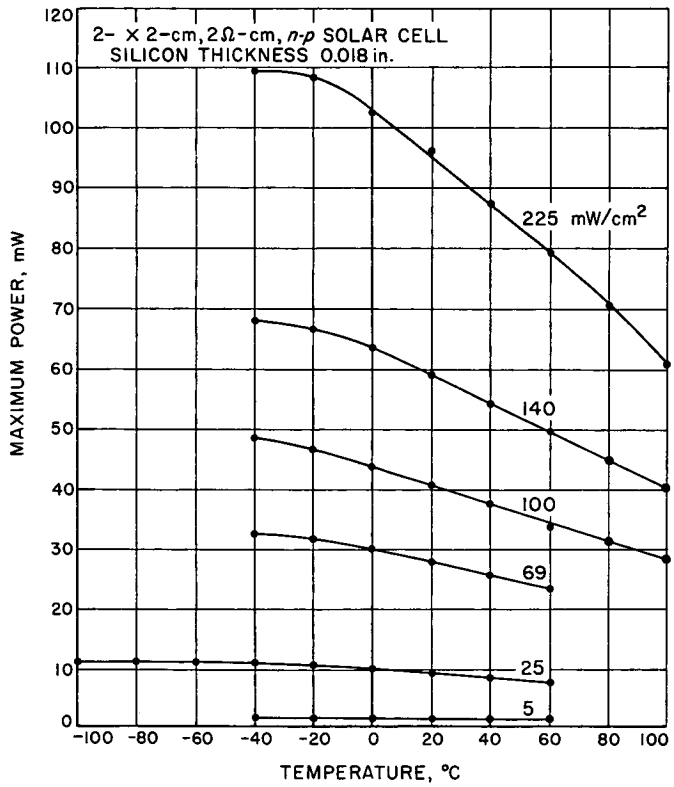

Fig. 10. Maximum power as a function of temperature for 18-mil single-crystal solar cell

The maximum power (P_{max}) as a function of cell temperature for the various type solar cells investigated in this evaluation is presented in Figs. 6, 10, 14 and 18. The increase in P_{max} with decreasing temperature is approximately linear down to 0°C for each type solar cell investigated. Below this temperature, the power rolls

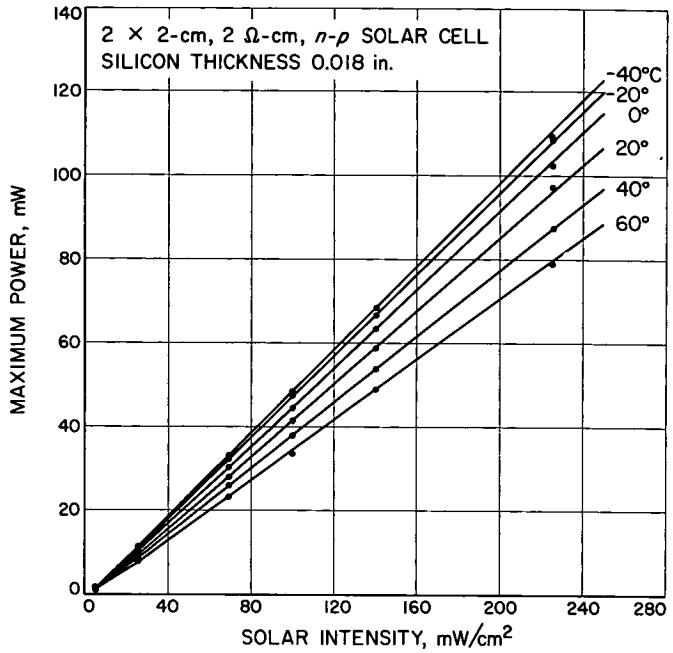

Fig. 11. Maximum power as a function of solar intensity for 18-mil single-crystal solar cell

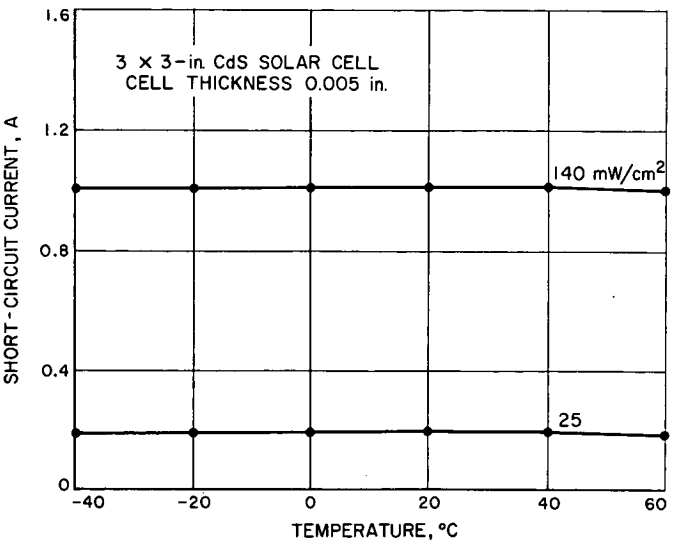

Fig. 12. Short-circuit current as a function of temperature for dendritic silicon solar cell

off and becomes essentially constant for temperatures below −50°C. That is, the cells appear to approach a constant power source below −40°C. The maximum power decreases at a nominal rate of approximately 0.4%/°C for the single-crystal silicon cells, 0.4%/°C for the webbed dendritic, and 0.3% for CdS above 0°C at an equivalent solar intensity of 140 mW/cm². The P_{max} as a function of solar intensity for the 8- and 18-mil n-p silicon, dendritic silicon, and CdS solar cells are shown in Figs. 7, 11, 15, and 19, respectively. The maximum power increases linearly with increasing intensity for any given temperature for each of the cell types investigated in this analysis.

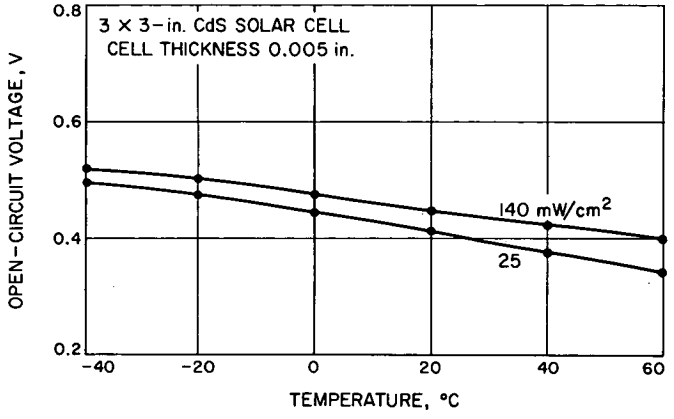

Fig. 13. Open-circuit voltage as a function of temperature for dendritic silicon solar cell

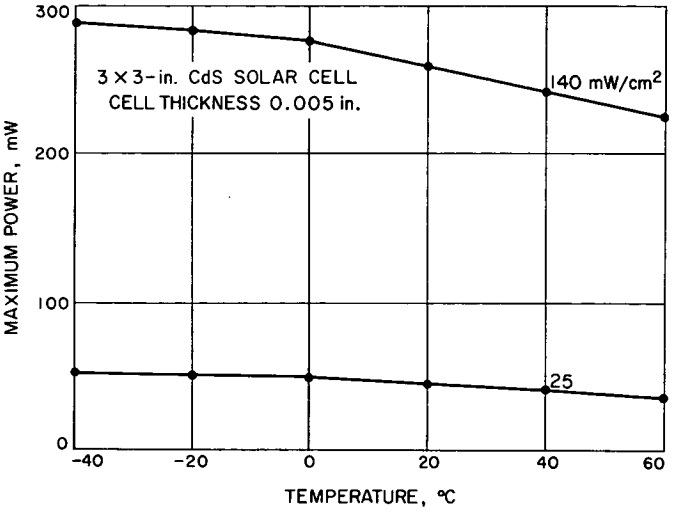

Fig. 14. Maximum power as a function of temperature for dendritic silicon solar cell

The efficiency as a function of temperature for the 8- and 18-mil single-crystal silicon, dendritic silicon, and CdS solar cell are presented by Fig. 20 at AM0.

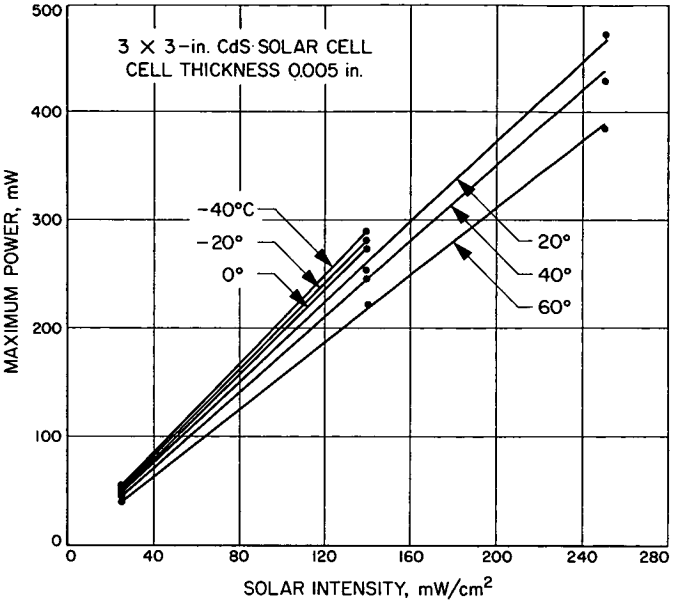

Fig. 15. Maximum power as a function of solar intensity for dendritic silicon solar cell

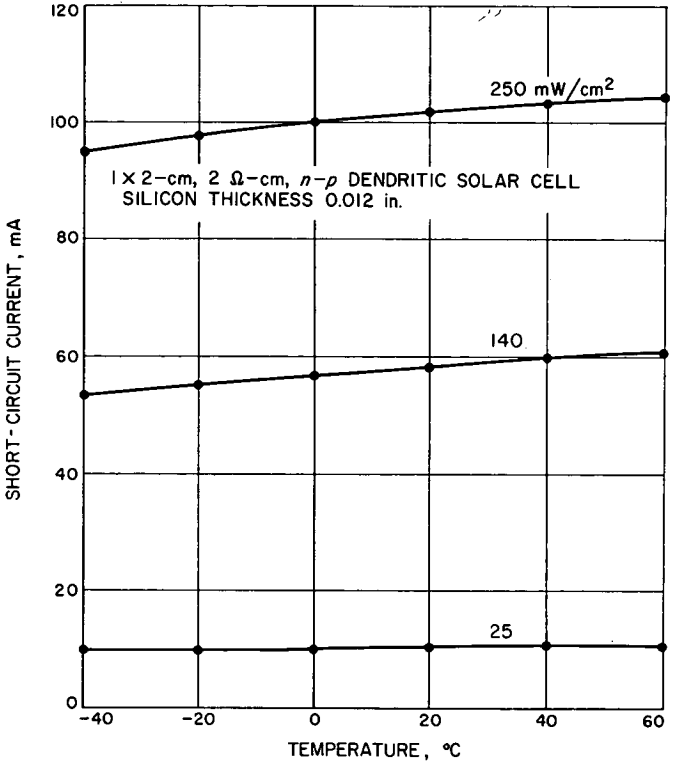

Fig. 16. Short-circuit current as a function of temperature for CdS solar cell

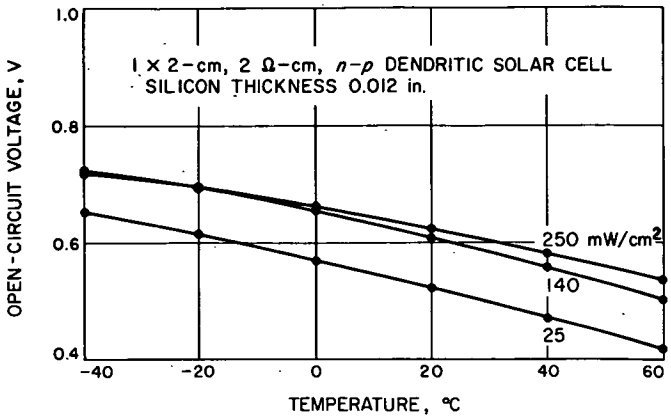

Fig. 17. Open-circuit voltage as a function of temperature for CdS solar cell

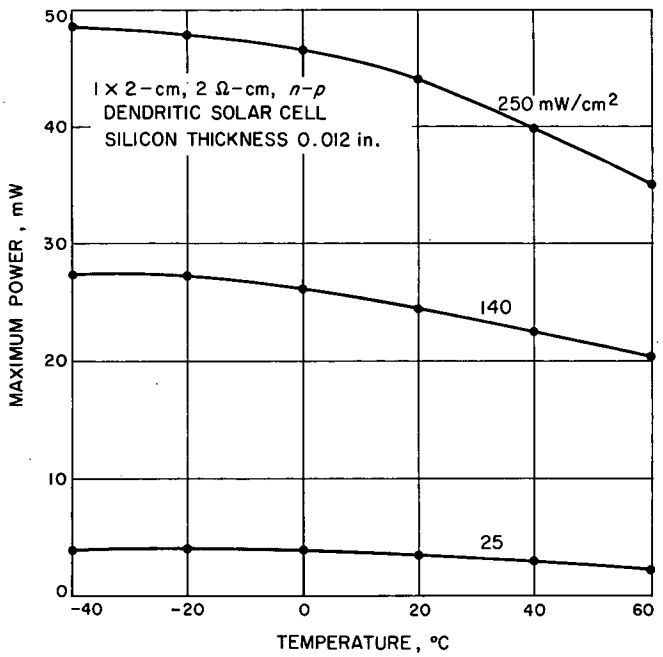

Fig. 18. Maximum power as a function of temperature for CdS solar cell

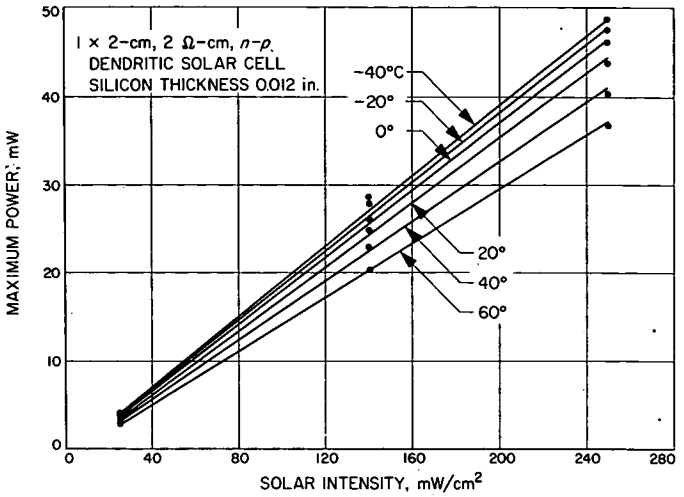

Fig. 19. Maximum power as a function of solar intensity for CdS solar cell

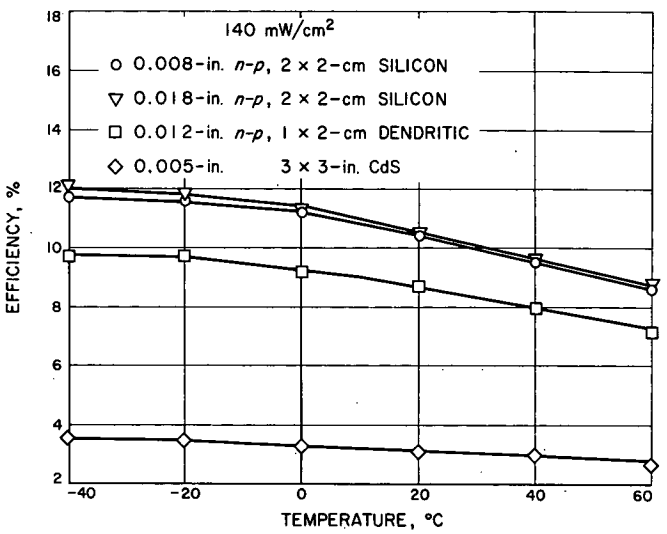

Fig. 20. Solar cell efficiency as a function of cell temperature

The percentage decrease in efficiency for all the cell types, as the temperature is increased, is essentially equal. The efficiency as a function of solar intensity, for each type cell investigated herein, is given by Fig. 21 at 60 and 0°C. Notice that the efficiency of the 8-mil cell appears better at low intensity levels than does the 18-mil cell. These efficiency numbers are based on the assumption that the 8-mil and 18-mil cells have front surface areas of 4 cm^2; the dendritic cells have an active area of 2 cm^2; and the CdS type cells have an active area of 58 cm^2.

V. Solar Array Applications

When considering the application of the developmental type cells discussed in this paper, the design engineer must consider the many tradeoffs in using the new type cells. Some of these are area utilization, efficiency, power requirements, lifetime, reliability, and costs. The relative importance of each of these parameters must be considered relative to the spacecraft mission criteria.

Increased interest has recently been directed toward the CdS type solar cell and its application to high-power

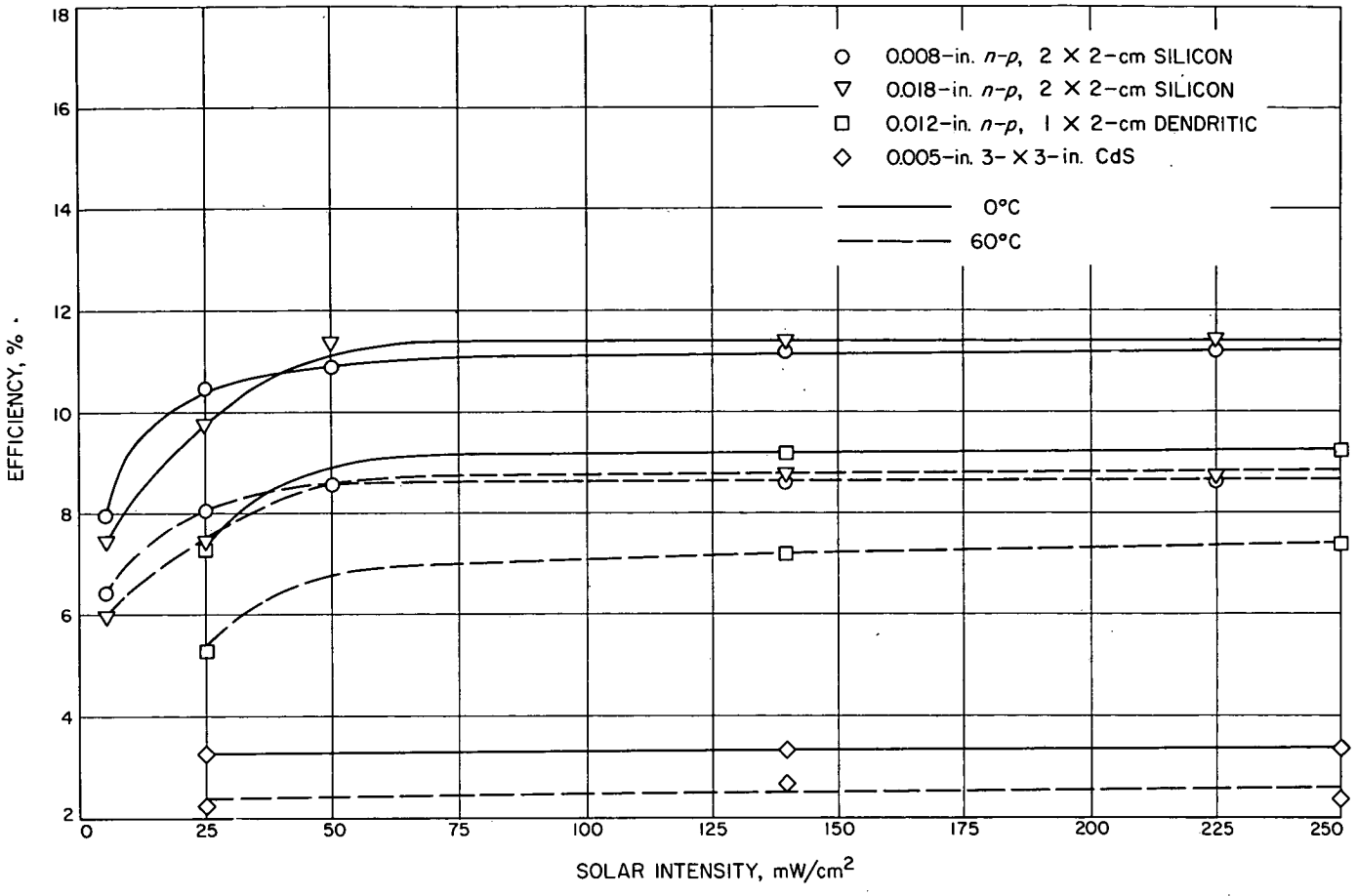

Fig. 21. Solar cell efficiency as a function of solar intensity

solar arrays. As indicated in the data presented earlier, the efficiency of the CdS cell at AM0 environment is low enough to require three times the area of a silicon cell for an equal power output. This factor should be considered by the design engineer, since this fact could pose serious implications to spacecraft attitude-control systems and methods of deployment. Studies have been conducted indicating optimism concerning the CdS solar cell when compared with the silicon solar cell. However, the data obtained under this test program indicate that the W/lb of 0.008 in silicon cell (including interconnectors and 3-mil bonded coverglass), is equal to the W/lb of the CdS type cell—which shows no advantage to the CdS type cell.

It presently appears that the only significant advantages of the CdS film cell are (1) the radiation-resistance characteristics and (2) the ease of manufacturing into solar arrays. The CdS cell without the need for coverglass protection against low-energy particles and the 3- × 3-in. size of the cell tend to minimize handling and assembly cost of arrays. The assembly of CdS film cells into arrays that will meet rigorous flight requirements and testing has not been accomplished to date, meeting stringent requirements could influence the assembly costs.

When considering the application of either dendritic solar cells, or large area single-crystal silicon solar cells to solar arrays, the aspects of reliability must be studied. Present designs of arrays use either the 1- × 2-cm or the 2- × 2-cm type cell and are arranged in matrices of series and parallel sets of cells. From use of the larger type cells, some disadvantages may arise in the lower power ranges of operations, depending upon the series parallel arrangement and the mechanism of failure. Advantages of the larger-area type cell are the implication on panel assembly and handling and the resultant possible cost advantages. These aspects must be considered in more detail as to replacement problems and handling damage before realistic trends can be established.

Through the past 10 yr, much experience has been gained in the processing of solar cells and the fabrication of solar arrays. For instance JPL has, since 1959, procured over 700,000 solar cells of various types, and assembled these into arrays. One area of problems that has been common on all of these programs is associated with solar cell electrical contacts. Earlier, the cell contact consisted of electroless nickel plating; today there is the silver-titanium contact on silicon solar cells. Both of these contacts have been proven to be inadequate under certain environmental conditions and when employed with certain solar array fabrication techniques. As an example, the silver-titanium, solder-dipped type of cell, when cycled through temperature extremes of −196 to 135°C, appears to suffer severe stress between the contact and silicon, causing silicon breakage or contact delamination as shown in Figs. 22 and 23. It is felt that further cell contact development must be initiated to improve contact ruggedness.

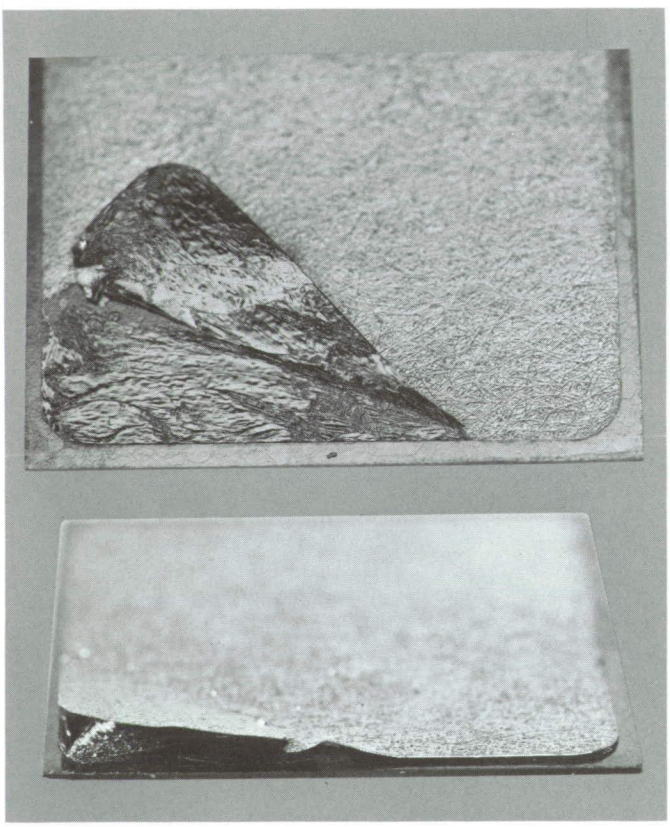

Fig. 22. Contact delamination and bulk silicon peel

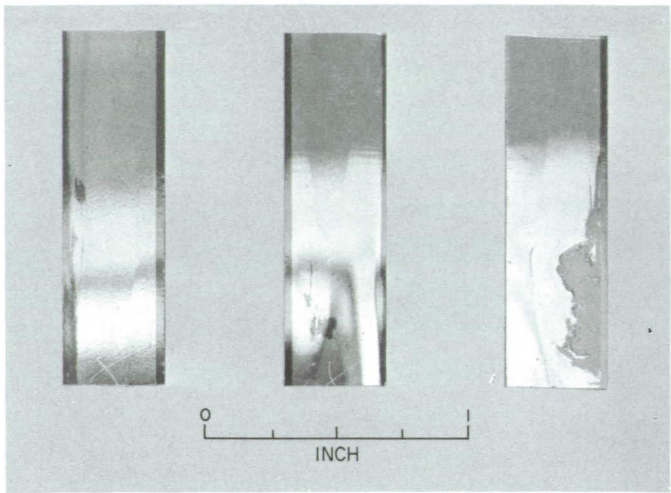

Fig. 23. Contact voids and silver scavenging

VI. Summary

The data obtained on developmental solar cells from this study demonstrate the electrical ability of these types of cells at temperature and intensities in the space equivalent regions of Venus and Jupiter. Also the data indicate that the single-crystal silicon solar cell exhibits advantages over the CdS developmental type solar cell. The variation in silicon thickness of the single-crystal solar cells tested under this program indicated better performance for thinner cells at equivalent solar intensities below 30 mW/cm^2, apparently due to lower shunt resistance associated with the thicker cells. The state-of-the-art type single-crystal silicon solar cell is being approached in efficiency by the webbed dendritic type solar cell. However, both types of cells exhibit problems with the silver-titanium contact, either solder coated or solderless.

The data generally support the silicon solar cell for most spacecraft missions anticipated in the future. However, environmental test programs should be initiated to increase confidence in these devices at extreme environments. To consider the CdS type solar cell in the future, it appears that the efficiency must be at least doubled to be fully competitive with the silicon devices.